Genome-wide CRISPR-based gene knockout screens reveal cellular factors and pathways essential for nasopharyngeal carcinoma

Received for publication, April 10, 2019, and in revised form, April 26, 2019 Published, Papers in Press, May 9, 2019, DOI 10.1074/jbc.RA119.008793

Chong Wang[‡], Sizun Jiang[‡1], Liangru Ke[§], Luyao Zhang[‡], Difei Li[‡], Jun Liang[‡], Yohei Narita[‡], Isabella Hou[‡], Chen-hao Chen[¶‖], Liangwei Wang[‡], Qian Zhong[‡§], Yihong Ling[§], Xing Lv[§], Yanqun Xiang[§], Xiang Guo[§], Mingxiang Teng[**], Sai-Wah Tsao[‡‡], Benjamin E. Gewurz[‡], Mu-Sheng Zeng[§2], and Bo Zhao[‡3]

From the [‡]Division of Infectious Disease, Department of Medicine, Brigham and Women's Hospital and Harvard Medical School, Boston, Massachusetts 02115, the [§]State Key Laboratory of Oncology in South China, Collaborative Innovation Center for Cancer Medicine, Guangdong Key Laboratory of Nasopharyngeal Carcinoma Diagnosis and Therapy, Sun Yat-sen University Cancer Center, Guangzhou 510060, China, the [¶]Center for Functional Cancer Epigenetics, Dana-Farber Cancer Institute, Boston, Massachusetts 02115, the [‖]Department of Biostatistics and Computational Biology, Dana-Farber Cancer Institute and Harvard School of Public Health, Boston, Massachusetts 02115, the [**]Department of Biostatistics and Bioinformatics, H. Lee Moffitt Cancer Center and Research Institute, Tampa, Florida 33612, and the [‡‡]School of Biomedical Sciences and Center for Cancer Research, Li Ka Shing Faculty of Medicine, The University of Hong Kong, Hong Kong, China

Edited by Xiao-Fan Wang

Early diagnosis of nasopharyngeal carcinoma (NPC) is difficult because of a lack of specific symptoms. Many patients have advanced disease at diagnosis, and these patients respond poorly to treatment. New treatments are therefore needed to improve the outcome of NPC. To better understand the molecular pathogenesis of NPC, here we used an NPC cell line in a genome-wide CRISPR-based knockout screen to identify the cellular factors and pathways essential for NPC (*i.e.* dependence factors). This screen identified the Moz, Ybf2/Sas3, Sas2, Tip60 histone acetyl transferase complex, NF-κB signaling, purine synthesis, and linear ubiquitination pathways; and MDM2 proto-oncogene as NPC dependence factors/pathways. Using gene knock out, complementary DNA rescue, and inhibitor assays, we found that perturbation of these pathways greatly reduces the growth of NPC cell lines but does not affect growth of SV40-immortalized normal nasopharyngeal epithelial cells. These results suggest that targeting these pathways/proteins may hold promise for achieving better treatment of patients with NPC.

Nasopharyngeal carcinoma (NPC)[4] occurs in the nasopharynx that is behind the nose and above the oropharynx. Early diagnosis of NPC remains difficult because of a lack of specific symptoms and its hidden anatomic location. Advanced disease is still frequently seen at first diagnosis (1). Radiotherapy and chemotherapy are the most commonly used treatments for NPC. Despite recent improvement in NPC treatment, the prognosis for patients with metastasis is still poor. In 2008, more than 51,000 patients died from NPC worldwide (2, 3). Therefore, new targeted therapies that specifically inactivate aberrant NPC oncogenic pathways are needed to improve patient outcome.

NPC is a unique human malignancy in which Epstein–Barr virus (EBV) is found in almost all undifferentiated NPCs (4). EBV latent membrane protein 1 (LMP1) activation of NF-κB provides signals for cell survival (5). LMP2A activates the phosphatidylinositol 3 kinase (PI3K)/AKT pathway (6). EBV microRNAs can promote metastasis (7). It was initially thought that most NPCs express LMP1 (8). However, it has been reported recently that the detection of LMP1 expression in NPC is highly variable. Frequently, it is not detectable in NPC biopsies (9, 10). Instead, abundant activating mutations in the NF-κB signaling pathway were found in NPC exome-seq analyses (9, 10). Interestingly, NPCs with activating mutations in the NF-κB pathway often lack LMP1 expression, suggesting essential roles of NF-κB in NPC pathogenesis. Other factors linked to NPC pathogenesis include genetic predisposition and environmental factors. A genome-wide association study found that NPC associated loci include HLA and the CDKN2A–CDKN2B gene cluster (11).

NPC whole-exome sequencing found mutations in epigenetic modifying enzymes are one of the most frequent genetic alterations in NPC (9, 12). Patients with mutations in this pathway had worse prognosis (12). These mutations can alter the epigenetic landscapes in cancer cells (12–15). Epigenetic alter-

This work was funded by National Institute of Health Grants AI123420 and CA047006 (to B. Z.), P30CA076292 (to M. T.), AI137337 (to B. E. G.), and National Natural Science Foundation of China Grants 81830090 and 81520108022 (to M. Z.). B. E. G. is a Burroughs Wellcome career award in medical sciences recipient. The authors declare that they have no conflicts of interest with the contents of this article. The content is solely the responsibility of the authors and does not necessarily represent the official views of the National Institutes of Health.

This article contains Figs. S1–S5.

[1] Present address: Baxter Laboratory for Stem Cell Biology, Stanford University School of Medicine, Stanford, CA 94305.

[2] To whom correspondence may be addressed. E-mail: zengmsh@sysucc.org.cn.

[3] To whom correspondence may be addressed: Dept. of Medicine, Brigham and Women's Hospital, 181 Longwood Ave., Boston, MA 02115. Tel.: 617-525-2643; Fax: 617-525-4257; E-mail: bzhao@bwh.harvard.edu.

[4] The abbreviations used are: NPC, nasopharyngeal carcinoma; EBV, Epstein–Barr virus; MAGeCK, model-based analysis of genome-wide CRISPR-Cas9 knockout; MYST, Moz, Ybf2/Sas3, Sas2, Tip60; KAT, histone lysine acetyltransferase; PAM, protospacer adjacent motif; MTX, methotrexate; LUBAC, linear ubiquitination assembly complex; sgRNA, single guide RNA.

This is an open access article under the CC BY license.

© 2019 Wang et al. Published under exclusive license by The American Society for Biochemistry and Molecular Biology, Inc.

ations are usually reversible and epigenetic enzymes are ideal drug targets, therefore understanding the aberrant epigenetic alterations will not only help us understand the molecular pathogenesis, but also allow identification of potential novel therapies. The PI3K pathway is also frequently affected in NPC. Other frequent mutations include TP53 and CDKN2A/B (9, 10, 12). Even though these proteins are not ideal drug targets themselves, it is possible to target their regulatory element (enhancers) to silence their expression.

Recently developed Clustered regularly-interspaced short palindromic repeats (CRISPR) technology enables rapid identification of dependency factors for cancer cell growth and survival (16). Silencing of dependency genes will lead to cell growth arrest or death. Identification of dependency genes will not only provide new insight into the molecular pathogenesis, but also identify novel therapeutic targets.

In this manuscript, we identified NPC dependency genes using a genome-wide CRISPR screen. Using these approaches, we identified novel pathways essential for NPC cell growth and survival.

Results

NPC dependency genes

Genome-wide CRISPR screens were used to identify NPC genes essential for their growth and survival. C666-1 is an EBV-positive NPC cell line, and NP69 is a normal human nasopharyngeal epithelial cell line immortalized by SV40 T antigen (17, 18). Lentiviruses were first used to generate cell lines stably expressing CAS9. The genome-wide Brunello library was then used to transduce NPC and control cells at a multiplicity of infection of 0.3. Cells were selected with puromycin and allowed to grow for 28 days. Total genomic DNAs were purified from 40 million of each line, and the sgRNAs were PCR-amplified. The sgRNAs were deep-sequenced and mapped to the human genome (Fig. 1*A* and Fig. S1). We used model-based analysis of genome-wide CRISPR-Cas9 knockout (MAGeCK) to identify genes essential for C666-1 cell survival but dispensable for NP69 cells (19, 20). We identified 711 genes depleted in C666-1 cells but not in NP69 cells (Fig. 1*B*). Dependency genes include the Moz, Ybf2/Sas3, Sas2, Tip60 (MYST) histone lysine acetyltransferase (HAT) family members and genes involved in the NF-κB signaling pathway, purine synthesis, the linear ubiquitin pathway, and the TP53 pathway. Pathway analyses identified that ribosomes, basal transcription factors, EBV infection, autophagy, and the cell cycle were enriched in KEGG pathways (Fig. 1*C*).

MYST histone lysine acetyl transferases family members are essential for NPC cell growth

KAT7 and KAT8 belong to the MYST family lysine acetyltransferases (KATs). A CRISPR screen identified KAT7 and its associated proteins BRD1(BRPF2), MEAF6, KAT7(HBO1/MYST2), and BRPF1 as NPC dependency factors (Fig. 2*A*). BRD1 and BRPF1 are scaffold proteins that assemble the HAT complexes and bridge MEAF6 (21, 22). BRD1 and BRPF1 have bromodomain and plant homeodomain (PHD) zinc fingers. The PHD domains bind to histones, thus providing docking sites for KATs. MEAF6 is a member of several MYST complexes. However, its function is not well characterized. KAT7 assembles protein complexes with BRD1 or BRPF1, MEAF6, and ING4/5 or JADE1/2/3 to acetylate H4K12, H4K5, H4K8, and H3K14 (21, 22).

To further validate the results from the screen, two sgRNAs were used to knock out KAT7 in C666-1 cells; a second EBV-positive NPC cell line, C17 cells; and NP69 cells. The sgRNAs were packaged into lentiviruses, and cells transduced with the lentiviruses were selected with puromycin. After selection, the cells were seeded at 2×10^5/ml for C666-1 and C17 cells and 5×10^4/ml for NP69 cells and allowed to grow. Western blotting showed very efficient knockout in all three lines tested (Fig. 2*B*). KAT7 knockout significantly decreased C666-1 and C17 cell growth ($p < 0.001$) but did not affect NP69 cell growth (Fig. 2*B*). To rule out CRISPR off-target effects, cDNA rescue was used. The KAT7sg1 PAM site in V5-tagged KAT7 rescue cDNA was mutated; thus, CAS9 would not be able to cut the cDNA. C17 cells were transduced with lentiviruses expressing KAT7sg1, alone or together with KAT7 rescue cDNA. KAT7 sgRNA efficiently reduced C17 cell growth. In contrast, the growth of cells expressing KAT7 rescue cDNA was comparable with that of cells expressing nontargeting sgRNA. The expression of rescue cDNA was validated by Western blotting (Fig. 2*C*). Cell cycle analyses found that NPC cells were growth-arrested in G_2/M phase (Fig. 2*D*). qRT-PCR was used to determine the effect of KAT7 knockout on the expression of genes essential for NPC. KAT7 knockout significantly reduced CHUK, GART, MDM2, RBCK1, SLC2A1, ATIC, and IKBKG expression in C666-1 cells (Fig. 2*E*; *, $p < 0.05$; **, $p < 0.01$). KAT7 knockout significantly reduced BRD1, IKBKB, MDM2, OTULIN, RBCK1, ATIC, IKBKG, and PIK3C3 expression in C17 cells (Fig. 2*F*; *, $p < 0.05$; **, $p < 0.01$). KAT7 knockout significantly reduced CHUK, IKBKB, MDM2, and RBCK1 expression in NP69 cells (Fig. 2*G*; *, $p < 0.05$; **, $p < 0.01$). These data suggest that KAT7 can contribute NPC cell growth and survival through up-regulation of NPC-essential genes.

To validate the effect of BRD1 knockout on NPC cell growth, two sgRNAs were used to knock out BRD1 in C666-1, C17, and NP69 cells. CRISPR efficiently reduced BRD1 expression in all three cell lines (Fig. 2*J*). BRD1 knockout significantly reduced C666-1 and C17 cell growth (**, $p < 0.01$) but did not affect NP69 cell growth (Fig. 2*I*). BRD1 expression levels in NPC tissues were also significantly higher than in non-NPC tissues by RNA-Seq ($p = 0.0079$) (Fig. 2*J*).

To validate the effect of MEAF6 knockout on NPC cell growth, two sgRNAs were used to knock out MEAF6 in C666-1, C17, and NP69 cells. CRISPR efficiently reduced MEAF6 expression in all three cell lines (Fig. 2*K*). MEAF6 knockout significantly reduced C666-1 and C17 cell growth (**, $p < 0.01$) but did not affect NP69 cell growth (Fig. 2*L*).

KAT8(MOF/MYST1) is also a member of the MYST family lysine acetyltransferases (Fig. 3*A*). Two sgRNAs were used to knock out KAT8 to test their ability to repress NPC cell growth. sgRNAs efficiently depleted KAT8 protein in all cell lines tested (Fig. 3*B*). KAT8 sgRNAs greatly decreased C666-1 and C17 cell growth (**, $p < 0.01$) and only slightly affected NP69 cell growth (Fig. 3*C*, $p > 0.05$).

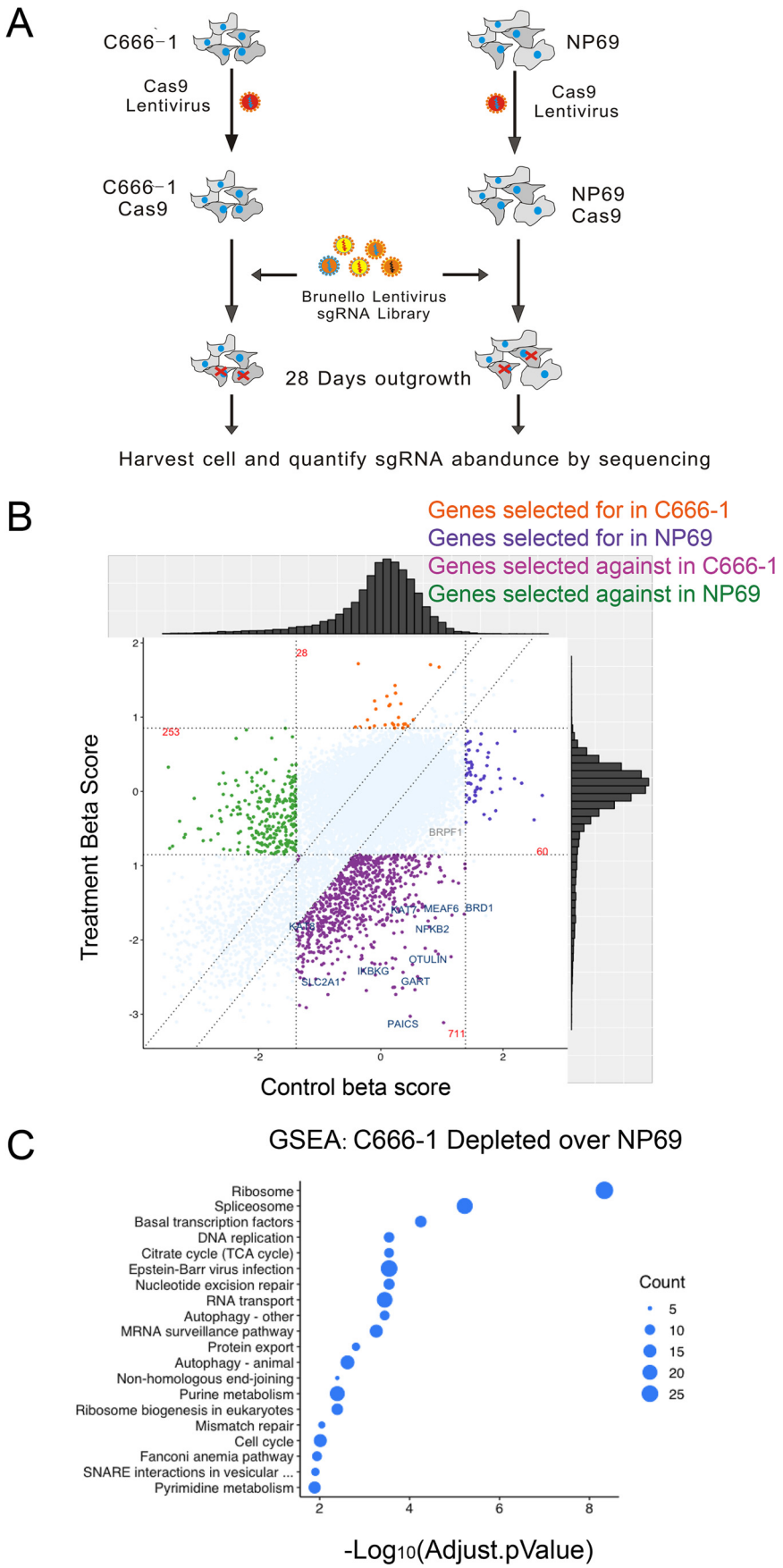
A
C666−1
Cas9
Lentivirus
NP69
Cas9
Lentivirus
C666−1
Cas9
NP69
Cas9
Brunello Lentivirus
sgRNA Library
28 Days outgrowth
Harvest cell and quantify sgRNA abandunce by sequencing
B
Genes selected for in C666-1
Genes selected for in NP69
Genes selected against in C666-1
Genes selected against in NP69
Treatment Beta Score
Control beta score
28
253
60
711
BRPF1
MEAF6
BRD1
NFKB2
OTULIN
IKBKG
GART
SLC2A1
PAICS
C
GSEA: C666-1 Depleted over NP69
Ribosome
Spliceosome
Basal transcription factors
DNA replication
Citrate cycle (TCA cycle)
Epstein-Barr virus infection
Nucleotide excision repair
RNA transport
Autophagy - other
MRNA surveillance pathway
Protein export
Autophagy - animal
Non-homologous end-joining
Purine metabolism
Ribosome biogenesis in eukaryotes
Mismatch repair
Cell cycle
Fanconi anemia pathway
SNARE interactions in vesicular ...
Pyrimidine metabolism
Count
5
10
15
20
25
-Log10(Adjust.pValue)

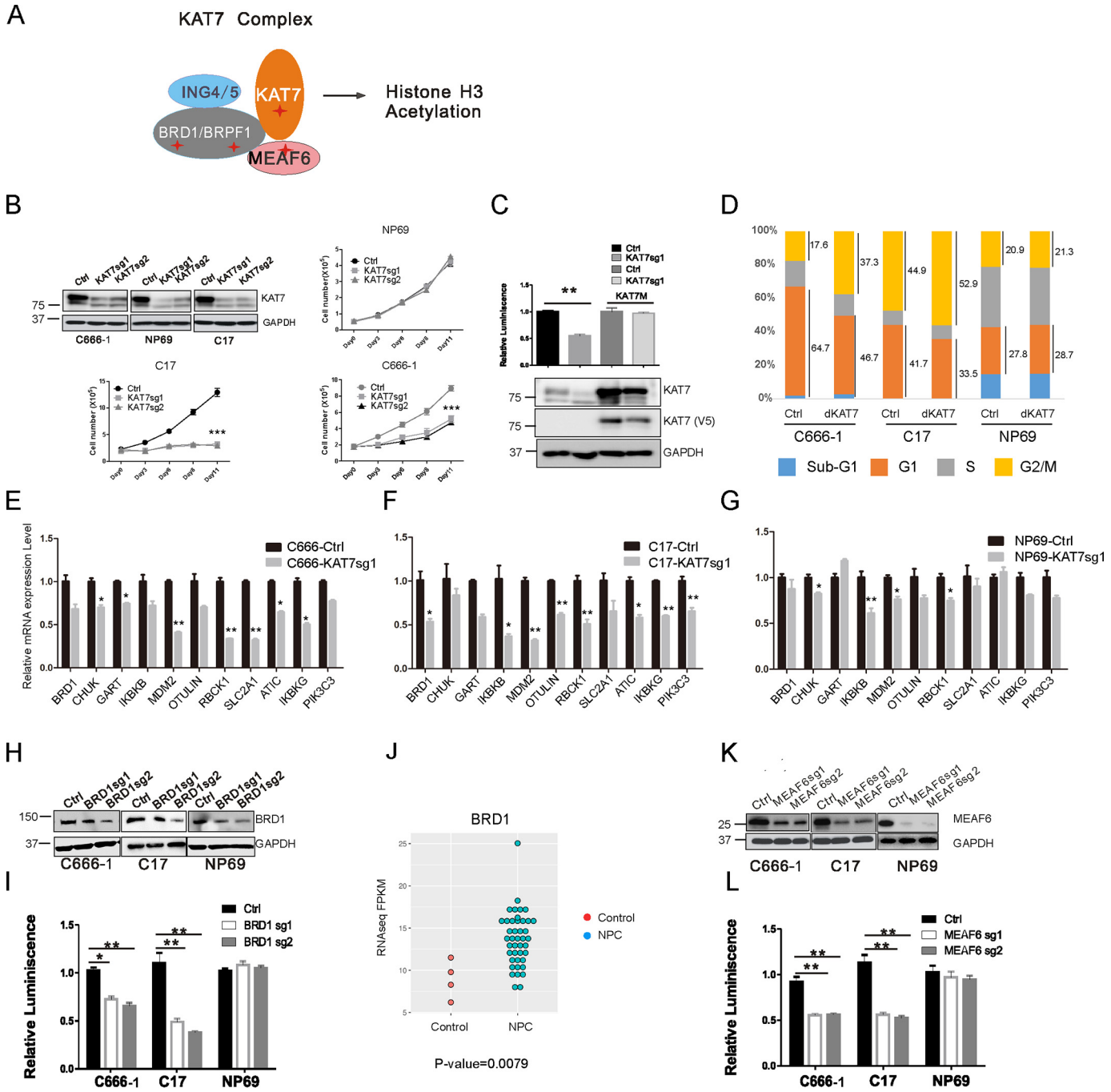

Figure 2. MYST histone lysine acetyl transferase family members are essential for NPC cell growth and survival. *A*, cartoon representing components of the KAT7 complexes. *Stars* indicate CRISPR hits with significant β scores. *B*, C666-1, C17, and NP69 cells were infected with lentiviruses expressing control (*Ctrl*) or sgRNAs against KAT7. Cells were seeded after puromycin selection. KAT7 expression is shown in Western blotting with GAPDH as a loading control. The cell numbers were counted on the indicated day (***, $p < 0.001$). *C*, lentivirus-transduced, V5-tagged KAT7 cDNA with the KAT7sg1 PAM site mutated (KAT7M) was used to rescue the KAT7 knockout. Luminescent cell viability assay was used to measure cell growth after endogenous KAT7 knockout in control or KAT7 rescued cells (**, $p < 0.01$). Western blots were used to confirm endogenous and V5-tagged rescue KAT7 expression. *D*, cell cycle analyses of cells with KAT7 knockout. *E*, qRT-PCR analyses of NPC dependence factor expression after KAT7 knockout in C666-1 cell. Control sgRNA levels were set to 1 (**, $p < 0.01$; *, $p < 0.05$). *F*, qRT-PCR analyses of NPC dependence factor expression after KAT7 knockout in C17 cells. Control sgRNA levels were set to 1 (**, $p < 0.01$; *, $p < 0.05$). *G*, qRT-PCR analyses of NPC dependence factor expression after KAT7 knockout in NP69 cell. Control sgRNA levels were set to 1 (**, $p < 0.01$; *, $p < 0.05$). *H*, BRD1 expression after knockout. *I*, cell growth following BRD1 knockout (**, $p < 0.01$; *, $p < 0.05$). *J*, BRD1 expression level in NPC tissue and non-NPC tissues. *K*, MEAF6 expression after knockout. *L*, cell growth following MEAF6 knockout (**, $p < 0.01$).

Figure 1. Genome-wide CRISPR screen for NPC dependency factors. *A*, CRSIPR knockout experimental design. *B*, β scores from the CRISPR screen of control (NP69 cells) *versus* treatment (C666-1 cells). Genes with a deviation of 2.5 × S.D. from the normalized mean β scores are highlighted, with positive β scores meaning selected for and negative β scores selected against. Top-scoring genes as well as genes of interest are highlighted. *C*, top GSEA categories for gene sets preferentially depleted in C666-1 cells compared with NP69 cells. The size of the *spheres* is proportional to the normalized enrichment scores.

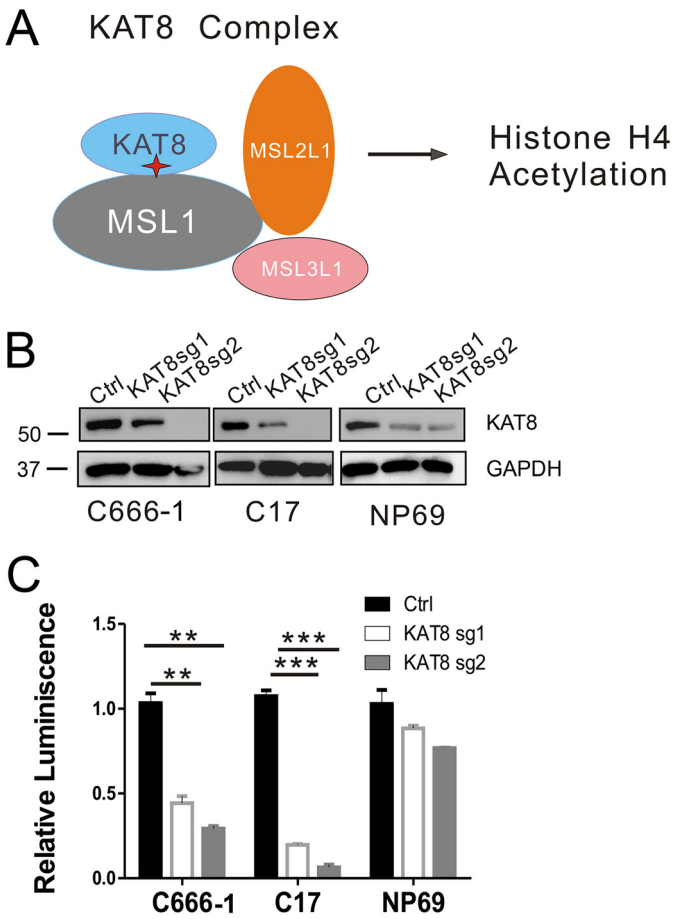

Figure 3. KAT8 is essential for NPC. *A*, cartoon representing components of the KAT8 complexes. The *star* indicates CRISPR hits with significant β scores. *B*, KAT8 expression after knockout. *C*, cell growth following KAT8 knockout (***$p < 0.001$, **$p < 0.01$).

The NF-κB pathway is essential for NPC growth

NF-κB activity is usually very high in NPC (5). NF-κB is activated either by the EBV oncoprotein LMP1 or mutations in the NF-κB signaling pathway (9). The expression of LMP1 in C666-1 cells is very inconsistent (9). However, a CYLD frameshift mutation in C666-1 cells leads to complete loss of CYLD protein expression. Restoration of WT CYLD protein expression reduces NF-κB activity (9). sgRNAs for CHUK, IKBKB, and IKBKG were significantly depleted in C666-1 cells but not in NP69 cells (Fig. 4*A* and Fig. S2*A*). In addition, RELB, NFKB1, NFKB2, NFKBIA, TAK1, TRAF6, and TRAF4 were also essential for C666-1 growth and survival but not for NP69 cells (Fig. 4*A*). Both canonical and noncanonical NF-κB pathway proteins were essential for C666-1, suggesting that both pathways are activated in C666-1 cells (Fig. 4*A*). The effect of IKBKB small-molecule inhibitor VIII on C666-1 and NP69 growth was tested. The IKBKB inhibitor slightly reduced NP69 cell growth. In contrast, the IKBKB inhibitor significantly reduced C666-1 cell growth (***, $p < 0.001$; Fig. 4*B*). To further validate the effects of CRISPR knockout, two sgRNAs for CHUK were tested for their effects on cell growth. CRISPR knockout efficiently reduced gene expression in both C666-1 and NP69 cells (Fig. 4*C*). CRISPR knockout also significantly reduced C666-1 cell growth (**, $p < 0.01$) but had minimal effect on NP69 cell growth (Fig. 4*D*). CRISPR knockout efficiently reduced the IKBKB protein level and halted C666-1 cell growth (Fig. 4, *E* and *F*; ***, $p < 0.001$). IKBKG knockout greatly reduced the IKBKG protein level and reduced C666-1 cell growth, but it did not affect NP69 growth (Fig. 4, *G* and *H*; **, $p < 0.01$) These data indicated that NF-κB activity is essential for C666-1 cell growth.

Purine synthesis pathway is essential for NPC growth

sgRNAs targeting the purine synthesis pathway enzymes GART, ADSL, PAICS, and ATIC were significantly depleted in C666-1 cells (Fig. 5*A* and Fig. S3). To evaluate the importance of the purine synthesis pathway, we tested the effect of methotrexate (MTX) treatment on C666-1, C17, and NP69 cell growth. MTX can inhibit the enzymes involved in purine synthesis. At lower doses, MTX slightly inhibited the growth of all three cell lines. However, at higher doses, MTX greatly suppressed C666-1 and C17 growth while not further inhibiting NP69 cell growth (Fig. 5*B*). Two sgRNAs for ADSL were used to test the effect of knockout on C666-1, C17, and NP69 cell growth. CRISPR efficiently knocked out ADSL (Fig. 5*C*). C666-1 and C17 cell growth was significantly reduced, whereas NP69 cells grew normally (Fig. 5*D*). Two sgRNAs for GART were used to test the effect of knockout on C666-1, C17, and NP69 cell growth. CRISPR efficiently knocked out GART (Fig. 5*E*). C666-1 and C17 cell growth was significantly reduced, whereas NP69 cells grew normally (Fig. 5*F*). These data indicate that the purine synthesis pathway is important for NPC cell proliferation. Interestingly, the expression levels of these enzymes also correlated with a poorer prognosis in head and neck cancers (Fig. S3, *B–E*) (http://www.oncolnc.org/ (41)).[5]

SLC2A1 is essential for NPC growth

EBV LMP1 up-regulates SLC2A1 expression through NF-κB (23). shRNA knockdown of SLC2A1 in NP69 cells stably expressing LMP1 greatly reduces cell growth (23). SCL2A1 was identified as a dependency factor for C666-1 cells in our CRISPR screen. Two sgRNAs were used to test the effect of SLC2A1 knockout on C666-1 and NP69 cell growth. CRISPR efficiently reduced SLC2A1 expression, as shown by Western blotting (Fig. S4*A*). SLC2A1 CRISPR knockout greatly decreased C666-1 cell growth but had a minimal effect on NP69 cell growth (Fig. S4*B*). The effect of a SLC2A1 inhibitor, BAY876, on NPC cell growth was also evaluated. BAY876 inhibited C666-1 and C17 cell growth at around 100 nM. At this concentration, BAY876 had a minimal effect on NP69 cell growth. Increasing amounts of BAY876 further inhibited C666-1 and C17 cell growth. At higher concentrations, BAY876 also slightly decreased NP69 cell growth. However, the inhibitory effect of BAY876 on C666-1 and C17 was significantly stronger than on NP69 (Fig. S4*C*). These cells were also plated in medium with or without glucose. In the absence of glucose, C666-1 and C17 cells grew very poorly, whereas NP69 cells grew almost normally (Fig. S4*D*). These data further support the notion that SLC2A1 is important for NPC cell growth.

[5] Please note that the JBC is not responsible for the long-term archiving and maintenance of this site or any other third party–hosted site.

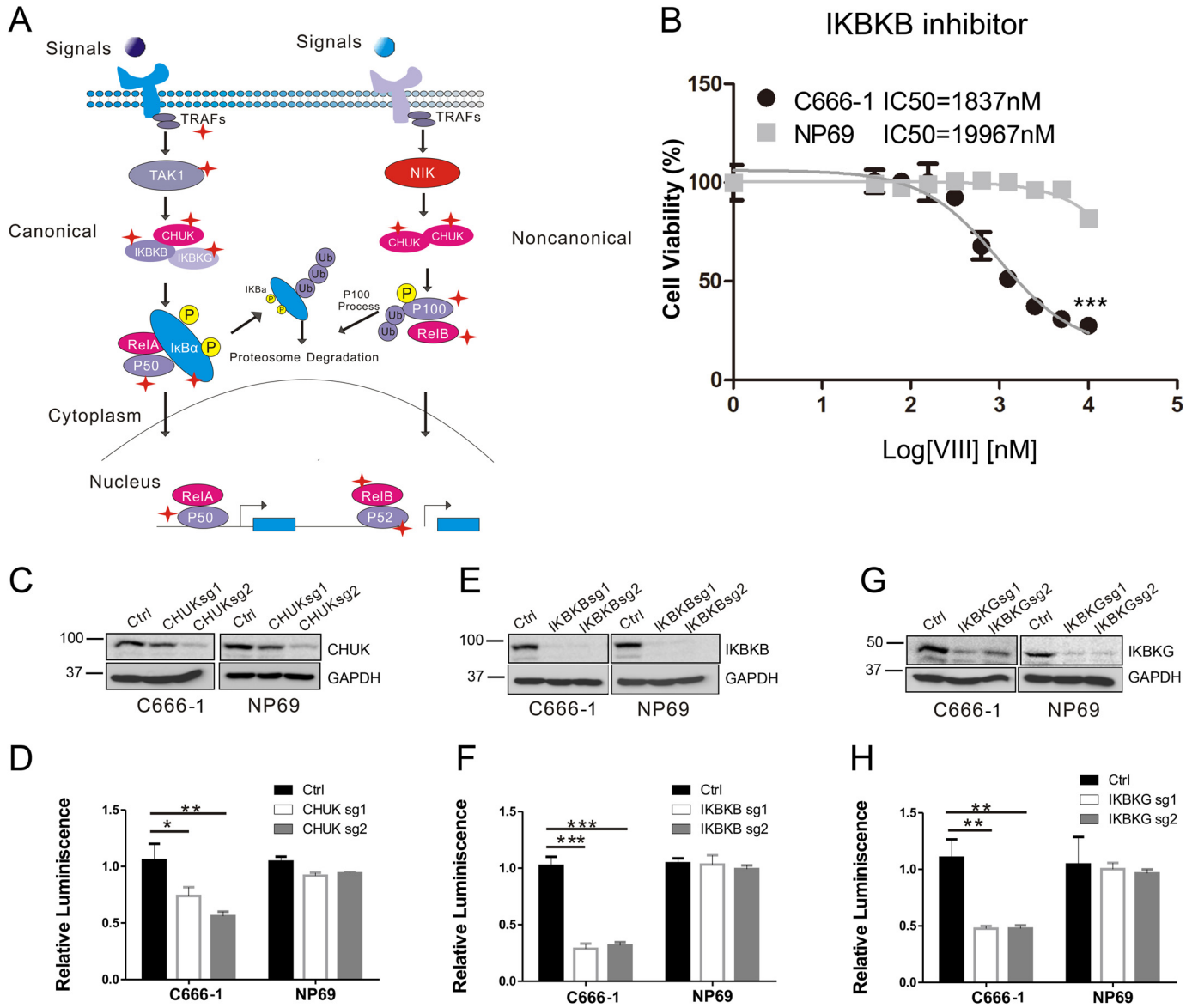

Figure 4. The NF-κB pathway is essential for NPC cell growth and survival. *A*, cartoon representing key components of the canonical and noncanonical NF-κB pathways is shown. Dependency factors are indicated by *stars*. *B*, C666-1 cells were treated with increasing amounts of IKBKB inhibitor for 3 days. Cell growth was determined by luminescent cell viability assay (***, $p < 0.001$). The IC_{50} values are indicated at the *top*. *C*, CHUK expression after knockout. *Ctrl*, control. *D*, cell growth following CHUK knockout (**, $p < 0.01$; *, $p < 0.05$). *E*, IKBKB expression after knockout. *F*, cell growth following IKBKB knockout (***, $p < 0.001$). *G*, IKBKG expression after knockout. *H*, cell growth following IKBKG knockout (**, $p < 0.01$).

Genes involved in regulating linear ubiquitin are important for NPC growth

The linear ubiquitination assembly complex (LUBAC) components RBCK, RNF31, and SHARPIN were all scored in the screen (Fig. 6*A*). LUBAC synthesizes linear polyubiquitin chains and plays a key role in NF-κB (24). To further validate the screen result, two sgRNAs were used to knock out RBCK1 to test their effects on C666-1 and NP69 growth. Knockout greatly reduced the protein level of RBCK1 (Fig. 6*B*). As expected, knockout of RBCK1 significantly decreased C666-1 cell growth (**, $p < 0.01$), whereas NP69 cell growth was unaffected (Fig. 6*C*). Two sgRNAs targeting RNF31 were also used to test their effects on C666-1 and NP69 cell growth. Knockout greatly reduced the protein level of RNF31 (Fig. 6*D*). Knockout of RNF31 significantly decreased C666-1 cell growth (**, $p < 0.01$), whereas NP69 cell growth was unaffected (Fig. 6*E*). These data suggest that LUBAC complexes are important for NPC cell growth. The LUBAC deubiquitinase OTULIN was also scored in the screen. OTULIN negatively regulates LUBAC activity. To test the effect of OTULIN depletion on C666-1 cell growth, two sgRNAs were selected to knock out OTULIN in C666-1 and NP69 cells. Knockout efficiently reduced OTULIN protein expression (Fig. 6*F*). OTULIN depletion greatly reduced C666-1 growth and had no effect on NP69 (Fig. 6*G*; **, $p < 0.01$). Because both the positive and negative regulators of linear ubiquitination were essential, the balance between the two events must be critical for NPC cell growth.

MDM2 and PIK3C3 are important for C666-1 cell growth

Tumor suppressor TP53 and PI3K pathway proteins are frequently mutated in NPC (9). Mutant TP53 can function as a dom-

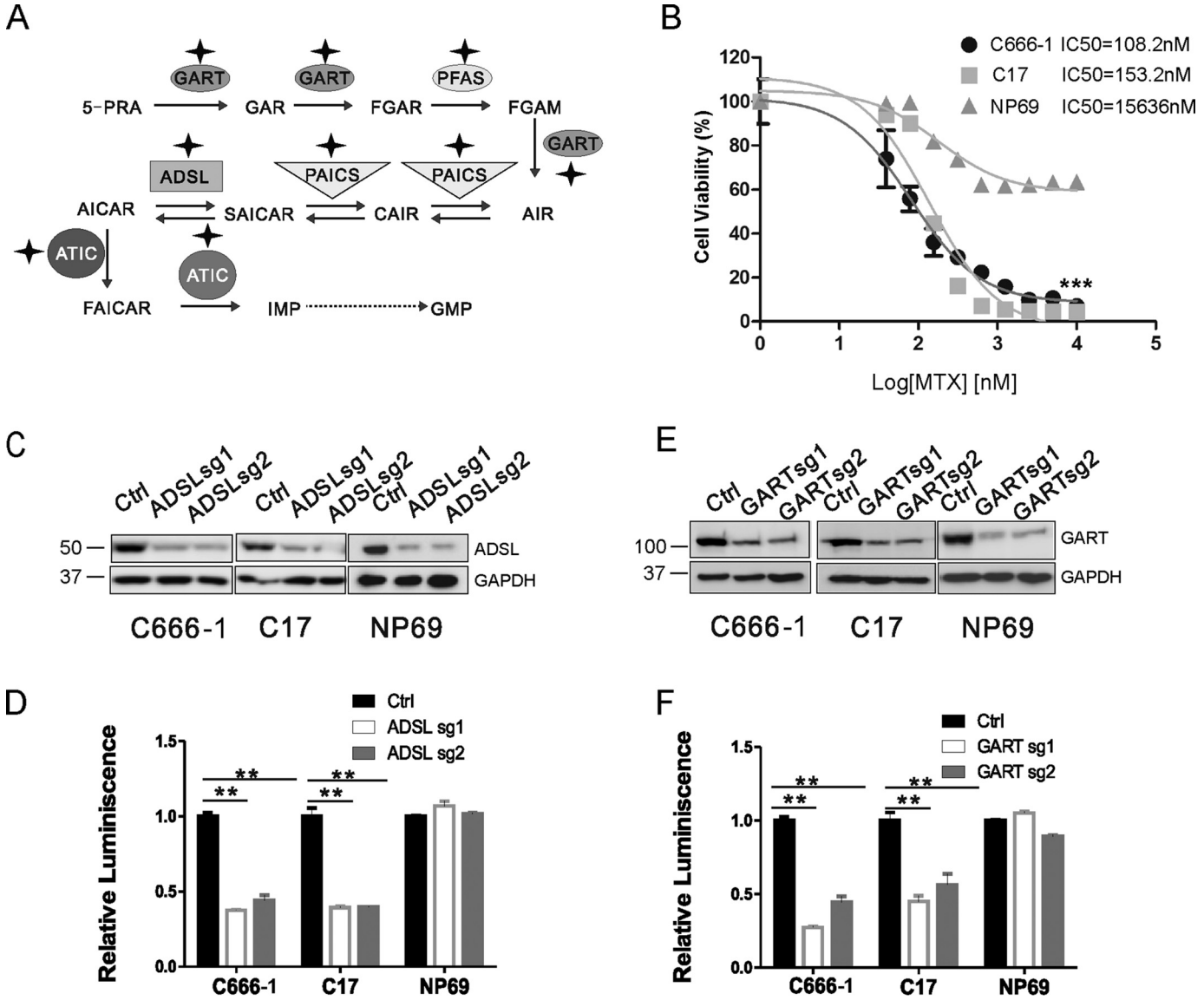

Figure 5. The purine synthesis pathway is essential for NPC cell growth and survival. *A*, the purine synthesis pathway. *Stars* indicate genes essential for NPC cell growth and survival identified by the CRISPR screen. *B*, NP69, C666-1, and C17 cells were treated with increasing amounts of MTX for 3 days. Cell growth was measured by luminescent cell viability assay (***, $p < 0.001$). The IC_{50} values are indicated. *C*, ADSL expression after knockout. *D*, cell growth following ADSL knockout (**, $p < 0.01$). *E*, GART expression after knockout. *F*, cell growth following GART knockout (**, $p < 0.01$).

inant negative for WT TP53, blocking its tumor suppressor function (25). MDM2 is an E3 ubiquitin ligase that is responsible for TP53 degradation (26). MDM2 was scored as an NPC dependency factor. Two sgRNAs targeting MDM2 efficiently knocked out MDM2 protein expression (Fig. 7*A*). Knockout also significantly decreased C666-1 cell growth while having a limited effect on NP69 cell growth (Fig. 7*B*). The MDM2 inhibitor Nutlin-3A significantly inhibited C666-1 cell growth while having less of an effect on NP69 cells (Fig. 7*C*; ***, $p < 0.001$). PIK3C3 was also scored as an NPC dependency factor. Two sgRNAs targeting PIK3C3 efficiently knocked out PIK3C3 protein expression (Fig. S5*A*). Knockout also significantly decreased C666-1 cell growth while having no effect on NP69 cell growth (Fig. S5*B*; **, $p < 0.01$).

Discussion

Recent advances in NPC treatment have greatly improved patient survival. However, 60% of patients have locoregional advanced disease or remote metastasis at diagnosis (1). These patients respond very poorly to treatments. Therefore, novel therapies specifically targeting NPC vulnerability are urgently needed.

A genome-wide CRISPR screen is a powerful tool to identity dependency factors essential for cell growth and survival (16). If there are drugs available for these dependency factors, then the effect of these drugs on NPC growth and survival can be tested easily. If these dependency factors are ideal drug targets, then it is possible to screen for specific inhibitors to develop new treatments. It is also possible to identify synthetic lethality targets.

C666-1 is a well-established EBV-positive NPC line derived from untreated patient xenografts. C17 is a newly derived EBV-positive NPC line originally derived from recurrent patient biopsy xenografts. NP69 is an SV40 T antigen immortalized normal nasopharyngeal epithelial cell line. We performed the

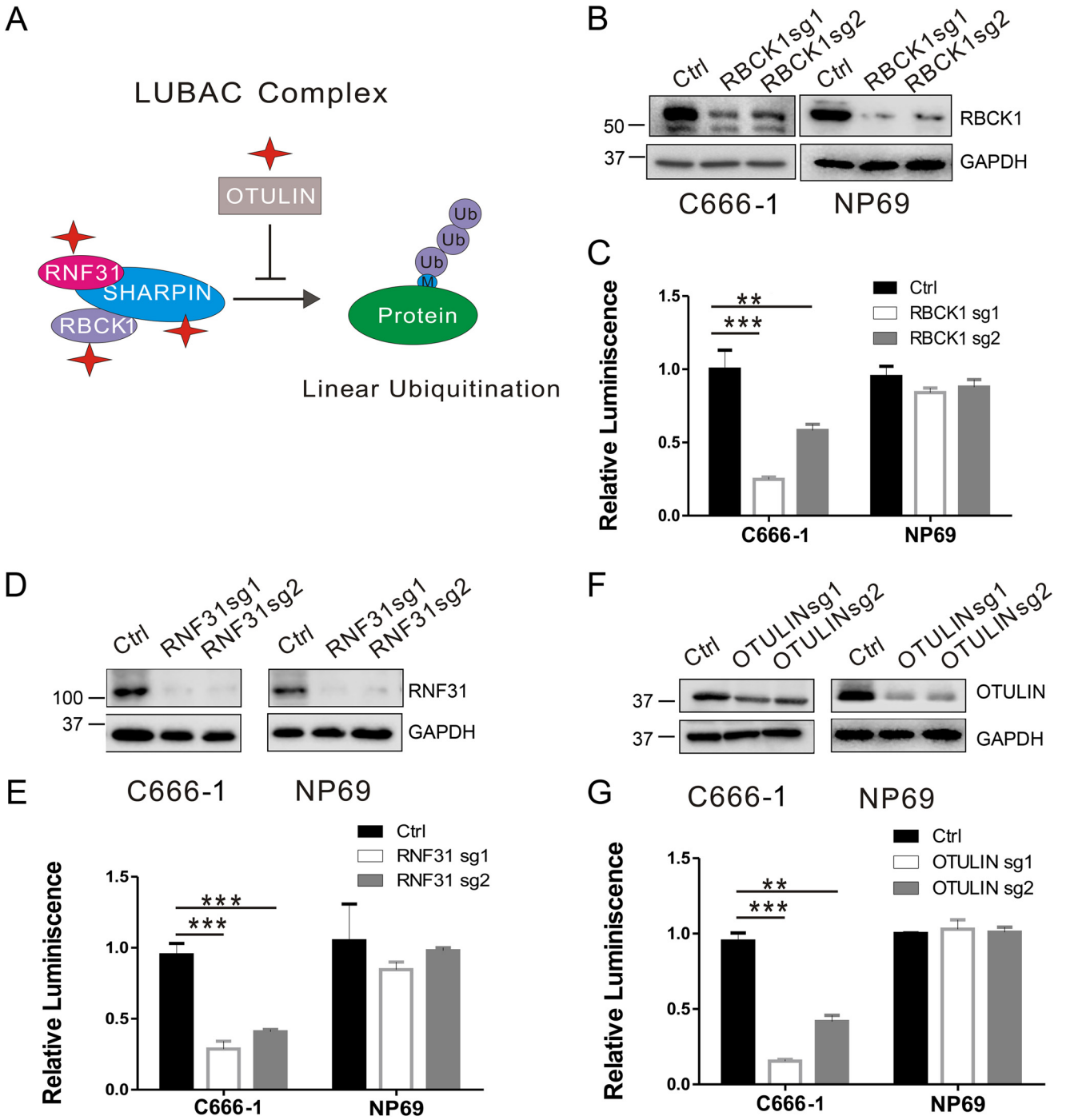

Figure 6. Linear ubiquitin is important for NPC cell growth and survival. *A*, cartoon representation of the linear ubiquitination pathway. NPC dependence factors are indicated by *stars*. *B*, RBCK1 protein expression after knockout. C, C666-1 and NP69 cell growth after RBCK1 knockout (***, $p < 0.001$; **, $p < 0.01$). *D*, RNF31 protein expression after knockout. *E*, C666-1 and NP69 cell growth followed by RNF31 knockout (***, $p < 0.001$). *F*, OTULIN protein expression after knockout. *G*, cell growth after OTULIN knockout (**, $p < 0.01$; ***, $p < 0.001$).

screen in C666-1 and NP69 cells to identify genes essential for C666-1 but dispensable for NP69 cells. We then validated some of the hits with the additional NPC cell line C17.

The MYST family of lysine acetyl transferases has four members: KAT5, KAT6A/B, KAT7, and KAT8. Both KAT7 and KAT8 were required for C666-1 and C17 cells but dispensable for NP69 cell growth and survival. A recently developed KAT6A inhibitor was effective in inducing senescence and inhibiting tumor growth (27). KAT7 can form complexes with different scaffold proteins to acetylate both H3K14 and H4K5, H4K8, and H4K12 (28). BRD1 can bridge histone and KATs (29). The BRD family member BRD4 is a well-characterized drug target that can specifically block cancer super-enhancers (SEs) (30). There is no small-molecule inhibitor that specifically blocks BRD1, even though a small-molecule inhibitor that inhibits both BRD1 and TAF1 is available. MEAF6 and BRPF1 were also scored in the screen and validated in both C666-1 and C17 cells. BRPF1 mutation causes defects in histone acetylation (31).

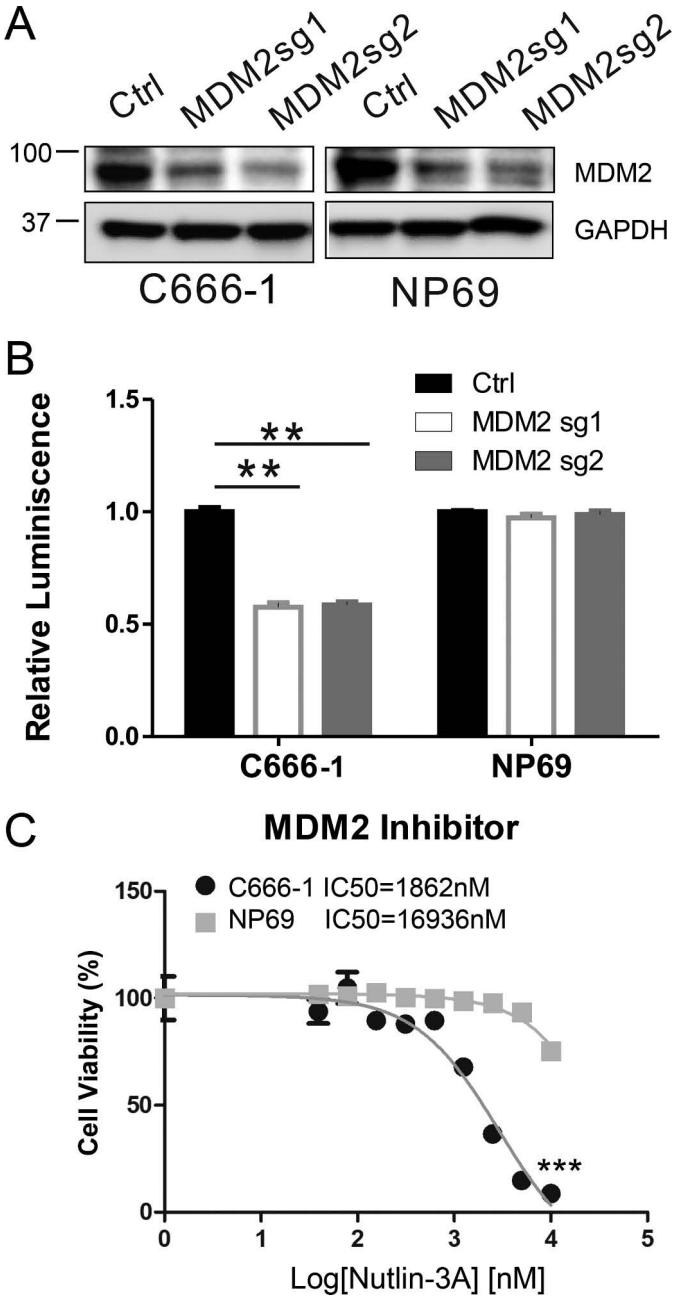

Figure 7. TP53 pathway is important for NPC cells. *A*, MDM2 protein expression after knockout. *B*, cell growth after MDM2 knockout (**, $p < 0.01$). *C*, MDM2 inhibitor Nutlin-3a significantly decreased C666-1 cell growth (***, $p < 0.001$). The IC_{50} values are indicated.

Because multiple components of the same pathway were scored in the screen, it is likely that this pathway is truly essential for NPC.

Multiple components of the NF-κB pathway were scored in the screen and validated in multiple NPC cell lines. These data further corroborate genetic studies that identified activating mutations in primary NPC biopsies (9). NF-κB provides survival signals to cancer cells (32). NPC SEs are enriched for NF-κB motifs, suggesting that NF-κB subunits are important transcription factors that cause SE formation (14). Interestingly, many of the NF-κB signaling molecules were also linked to NPC SEs. These may generate a positive feedback loop to increase NF-κB activity.

The purine synthesis pathway generates purine residues essential for DNA replication. MTX and methcapurine are older-generation drugs with great toxicity. MTX was used to treat NPC before in pediatric NPC and in combination with other chemotherapy drugs in adult NPC (33–35). If there is a newer generation of drugs available with less toxicity, or the potential to combine these drugs with other therapies, targeting this pathway may lead to improved patient outcomes.

Aerobic glycolysis (the Warburg effect) provides the additional energy needed for rapid cancer growth. The glucose transporter SLC2A1 transfers extracellular glucose into cancer cells. EBV LMP1 can increase SLC2A1 expression in both B cells and epithelial cells (23, 36). Our screen confirmed that SLC2A1 was essential for both C666-1 and C17 cell growth but dispensable for NP69 cells. Because the Warburg effect is seen in cancer cells but not in normal adult cells, targeting SLC2A1 may lead to a new therapy.

Linear ubiquitination provides another layer of regulation of the NF-κB pathway (24). Interestingly, factors enhancing linear ubiquitination and decreasing linear ubiquitination were both scored in the screen. These data suggest that the balance between the two signal components is critical for continuous NPC cell growth (37).

TP53 and PI3K pathways are frequently mutated in NPC (9). Our screen identified components of these two pathways to be essential for NPC cell growth. Even though it is difficult to target TP53 itself, it has been shown that it is possible to inactivate TP53 by regulating the activity of proteins responsible for degrading TP53 through the ubiquitination pathway. MDM2 is an TP53 E3 ubiquitin ligase. Small-molecule inhibitors are available to inactivate MDM2. PI3K pathway inhibitors are also under active investigation. It is possible that one of the inhibitors will have a great inhibitory effect on NPC cell growth.

We identified several pathways critical for NPC cell growth *in vitro*. Some are newly identified dependency factors, whereas others further corroborate previous studies. These NPC dependency factors are ideal targets for synthetic lethality studies. Because many of the existing NPC treatments are very toxic, selectively targeting NPC-specific pathways may lead to better therapies and improve treatment outcomes.

Experimental procedures

Cell lines

C666-1 and C17 are EBV-positive NPC cell lines (38). NP69 is a SV40 T antigen immortalized normal nasopharyngeal epithelial cell line. C666-1 and C17 cells were grown in RPMI 1640 medium supplemented with 10% fetal calf serum, 1 mM glutamine, 100 units/ml streptomycin, and 100 mg/ml penicillin. C17 cells were also supplemented with ROCK inhibitor Y-27632 at 4 μM. NP69 cells were grown in keratinocyte-SFM medium supplemented with epidermal growth factor and bovine pituitary extracts.

CRISPR screens

The C666-1 and NP69 cell lines were used for a genome-wide CRISPR screen to identify NPC-essential genes. The Brunello library containing sgRNAs targeting 19,114 host genes was obtained from Addgene (73178). The library was electropo-

rated into STBL4-competent cells for plasmid amplification. Extracted plasmids were then sequenced to measure the coverage distribution of sgRNAs per gene. More than 90% of the library was recovered in the amplification. The library was transfected with VSVG and PsPAX2 plasmids using TransIT transfection reagents (Mirus Bio) into four 150-mm dishes of 293T cells at 60% confluency. 24 h after transfection, cells were replenished with fresh medium to allow for lentiviral production. Lentiviruses were harvested twice, at 24 h and 48 h after medium change. For each replicate, 130 million Cas9-expressing C666-1 and NP69 cells were infected with lentiviruses at a multiplicity of infection of 0.3 to ensure that each cell received an average of one sgRNA containing virus. Infection was done in four 12-well plates per replicate. The cells were then spun at $300 \times g$ for 2 h at 30 °C in the presence of 4 μg/ml Polybrene to increase transduction efficiency. After infection, plates were returned to the 37 °C incubator for another 6 h before reseeding in a T175 large flask at 10% confluency. 48 h later, cells were selected with puromycin at 3 μg/ml. The medium was changed every 3 days, and cells were passaged once a confluency of 80% was reached. At least 40 million cells were passaged out each time to maintain adequate sgRNA library complexity.

After 28 days, cells were harvested, and genomic DNA was extracted by using the Blood and Cell Culture DNA Maxi Kit (Qiagen) according to the manufacturer's instructions. Extracted DNA was then used as a PCR template for sgRNA amplification. Multiple PCRs covering all genomic DNAs were performed according to protocols from the Broad Institute (https://portals.broadinstitute.org/gpp/public/resources/protocols).[5] Each PCR mixture contained 10 μg of genomic DNA, 1.5 μl of Ex Taq polymerase, 10 μl of 10× reaction buffer, 8 μl of dNTP, 0.5 μl of P5 primer mixture (100 μM), and 10 μl of P7 primer (5 μM) and was topped up to 100 μl with nuclease-free water. The PCR conditions were as follows: step 1, 95 °C for 1 min; step 2, 95 °C for 30 s; step 3, 53 °C for 30 s; step 4, 72 °C for 30 s; step 5, repeat steps 1–4 for a total of 28 cycles and a final extension at 72 °C for 10 min. Amplified sgRNAs were purified with AMPure XP-beads (Beckman Coulter) according to the manufacturer's instructions. Samples were then sequenced on the Illumina Nextseq platform (1 × 75 bp) at the Harvard Bauer Core Facility.

CRISPR screen analysis

Analysis of the CRISPR screen was performed with model-based analysis of genome-wide CRISPR-Cas9 knockout (MAGeCK) as described previously (19, 39). Downstream data visualization and β score cutoffs were done with MAGeCKFlute. Based on both biological replicates, a single β score for each gene was computed, and its distribution was normalized based on known essential genes to avoid experimental bias, such as different cell cycle progressions. For each gene, a positive β score indicates a positive selection, whereas a negative β score indicates negative selection. Differential β scores between C666-1 and NP69 cells were computed using a cutoff of 2.5 × S.D. around the mean β score of each condition. Genes that fell within each cutoff were counted and extracted. These genes fell into four groups: group 1 (selected for in C666-1 cells), group 2 (selected for in NP69 cells), group 3 (selected against in C666-1 cells), and group 4 (selected against in NP69 cells).

Pathway analysis using KEGG and GSEA was performed on differentially selected genes in each group. The β scores for each gene within the pathway for each condition were colored onto the KEGG Pathway map using Pathview (40).

CRISPR knockout

For hit validation, individual gene CRISPR knockout was performed with single sgRNAs from the Brunello library. In brief, sgRNAs targeting genes of interest were synthesized, annealed, and cloned into the pLentiGuide-Puro vector according to protocols from the Broad Institute. Cloned sgRNAs were packaged into lentiviruses exactly as described for the pooled CRISPR screen above. The harvested virus was filtered through a 0.45-μm filter before transducing the target cell. 48 h after infection, fresh medium containing 3 μg/ml puromycin was changed to select transduced cells for 3 days. Cells were then allowed to grow out for another 3–7 days before examining knockout efficiency by Western blotting and downstream assays.

Western blots

Cells were harvested and washed once with PBS, and cell pellets were resuspended with PBS. 6× SDS loading buffer was added to the cell suspension, followed by a brief sonication, and then boiled at 100 °C for 5 min before loading onto a SDS-PAGE gel. Protein was resolved by SDS-PAGE and transferred to an NC membrane at 100 V for 1 h. The membrane was then blocked with 5% nonfat milk with shaking at room temperature for 30 min and then incubated with a primary antibody targeting the protein of interest overnight at 4 °C. The next day, blots were washed with TBS-T (20 mM Tris, 150 mM NaCl, 0.1% Tween 20, pH 7.5) three times before incubation with HRP-labeled secondary antibody with shaking at room temperature for 1 h. Blots were developed with ECL chemiluminescence and imaged on a Carestream workstation.

cDNA rescue

cDNA rescue constructs in which protospacer adjacent motif (PAM) sequences of the sgRNA of interest were site-mutated to prevent Cas9 targeting while preserving protein amino acid sequence. DNA was synthesized by GenScript and cloned into the PLX-TRC313 vector, which contains a V5 tag and the hygromycin selection marker. Rescue and empty constructs were then packaged into lentiviruses as described above and used to infect target cells, followed by subsequent hygromycin selection. cDNA expression was confirmed by Western blotting for V5. Both control and rescue cDNA groups were used for further CRISPR knockout experiments with the sgRNA of interest. The sequences used for KAT7 are included in Table S1, with the mutated PAM sequences marked.

Cell growth assays

After 3 days of puromycin selection, cells were counted, and the same number of cells were seeded to attain ~10% confluency in 6 well plates. Cells were then allowed to grow out and passaged when they reach a confluency of 80% before harvest-

ing for cell number quantification. Growth curves were drawn based on the cell number obtained from each time point. A CellTiter-Glo® Luminescent Cell Viability Assay (Promega) was used to determine the relative number of viable cells under each condition, according to the manufacturer's instructions. Briefly, cells were harvested and resuspended with 1 ml of PBS in a 1.5 ml Eppendorf tube. 30 μl of cell suspension was drawn from each tube and transferred to a 96-well white plate. 30 μl of premixed CellTiter-Glo® reagent was added to the plate and shaken at room temperature for 2 min. Plates were then rested in a dark room for 10 min before spectral measurements with the SpectraMax workstation (Molecular Devices). Results are shown as relative luminescence normalized to the control group.

IC_{50}

Two days before treatment, cells were seeded into 96-well white plates at a concentration of 3000 cells/well for C666-1 and C17 cells or 1000 cells/well for NP69 cells. On day 0, media were replaced with fresh media containing the small inhibitors VIII (ApexBio, A3485), BAY876 (Sigma, SML1774–5MG), MTX (Sigma, A6770-100MG), and Nutlin3A (Sigma, SML0580-5MG). IC_{50} values were determined from dose–response curves from three replicates at each inhibitor concentration: 10 μM, 5 μM, 2.5 μM, 1.25 μM, 625 nM, 312.5 nM, 156.25 nM, 78.13 nM, and 39.06 nM. Cell growth was determined by CellTiter-Glo assay after treatment for 3 days. 0.1% DMSO was used for all controls.

Glucose withdrawal assay

NP69, C666-1, and C17 cells were first passaged and cultured with normal medium. Three days later, the medium was changed to RPMI 1640 medium containing 10% dialyzed FBS, 2 mM L-glutamine, and 100× penicillin–streptomycin (Gibco) in the presence or absence of 20 mM glucose. Cells were allowed to grow for another 3 days before pictures were taken under a bright-field microscope.

Statistical analysis

The MAGeCK approach and software package were used to identify essential genes from the CRISPR screes (19). In short, the read counts from the four samples (two cell lines, C666-1 and NP69, with two biological replicates each) were median-normalized based on sgRNA read counts. Next, sgRNA mean-variance modeling was performed using a negative binomial model to estimate the significance of each sgRNA in treatment and control samples. The sgRNAs were then ranked by their p values, and the gene essentiality was calculated with MAGeCK-mle.

The output of the above is a β score for each gene, where a positive β score indicates a positively selected gene (and, inversely, a negative β score indicates a negatively selected gene). This score is analogous to "log -fold change" used commonly in differential expression contexts. The β score allows direct comparison of experimental conditions. Finally, the β scores of previously identified genes indispensable for cell survival were used to normalize the β score distribution between the two conditions. Statistical significance calculated between treatment and control cells in growth assays were computed via a one-sided Student's t test.

Author contributions—C. W., S. J., L. Z., and M. T. data curation; C. W., D. L., J. L., and X. L. validation; C. W. and Y. X. investigation; C. W. and B. Z. writing-original draft; C. W. and B. Z. project administration; S. J. and C.-h. C. software; L. K., Y. N., L. W., Y. L., and M.-S. Z. resources; I. H. and X. G. writing-review and editing; Q. Z. conceptualization; S.-W. T. formal analysis; B. E. G. visualization; B. Z. funding acquisition.

Acknowledgment—We thank Elliott Kieff for insightful discussions.

References

1. Tang, X. R., Li, Y. Q., Liang, S. B., Jiang, W., Liu, F., Ge, W. X., Tang, L. L., Mao, Y. P., He, Q. M., Yang, X. J., Zhang, Y., Wen, X., Zhang, J., Wang, Y. Q., Zhang, P. P., *et al.* (2018) Development and validation of a gene expression-based signature to predict distant metastasis in locoregionally advanced nasopharyngeal carcinoma: a retrospective, multicentre, cohort study. *Lancet Oncol.* **19,** 382–393 CrossRef Medline
2. Jemal, A., Bray, F., Center, M. M., Ferlay, J., Ward, E., and Forman, D. (2011) Global cancer statistics. *CA Cancer J. Clin.* **61,** 69–90 CrossRef Medline
3. Raab-Traub, N. (2015) Nasopharyngeal carcinoma: an evolving role for the Epstein-Barr virus. *Curr. Top Microbiol. Immunol.* **390,** 339–363 Medline
4. Pathmanathan, R., Prasad, U., Sadler, R., Flynn, K., and Raab-Traub, N. (1995) Clonal proliferations of cells infected with Epstein-Barr virus in preinvasive lesions related to nasopharyngeal carcinoma. *N. Engl. J. Med.* **333,** 693–698 CrossRef Medline
5. Miller, W. E., Cheshire, J. L., Baldwin, A. S., Jr, and Raab-Traub, N. (1998) The NPC derived C15 LMP1 protein confers enhanced activation of NF-κB and induction of the EGFR in epithelial cells. *Oncogene* **16,** 1869–1877 CrossRef Medline
6. Fotheringham, J. A., Coalson, N. E., and Raab-Traub, N. (2012) Epstein-Barr virus latent membrane protein-2A induces ITAM/Syk- and Akt-dependent epithelial migration through αv-integrin membrane translocation. *J. Virol.* **86,** 10308–10320 CrossRef Medline
7. Cai, L., Ye, Y., Jiang, Q., Chen, Y., Lyu, X., Li, J., Wang, S., Liu, T., Cai, H., Yao, K., Li, J. L., and Li, X. (2015) Epstein-Barr virus-encoded microRNA BART1 induces tumour metastasis by regulating PTEN-dependent pathways in nasopharyngeal carcinoma. *Nat. Commun.* **6,** 7353 CrossRef Medline
8. Pathmanathan, R., Prasad, U., Chandrika, G., Sadler, R., Flynn, K., and Raab-Traub, N. (1995) Undifferentiated, nonkeratinizing, and squamous cell carcinoma of the nasopharynx: variants of Epstein-Barr virus-infected neoplasia. *Am. J. Pathol* **146,** 1355–1367 Medline
9. Li, Y. Y., Chung, G. T., Lui, V. W., To, K. F., Ma, B. B., Chow, C., Woo, J. K., Yip, K. Y., Seo, J., Hui, E. P., Mak, M. K., Rusan, M., Chau, N. G., Or, Y. Y., Law, M. H., *et al.* (2017) Exome and genome sequencing of nasopharynx cancer identifies NF-κB pathway activating mutations. *Nat. Commun.* **8,** 14121 CrossRef Medline
10. Zheng, H., Dai, W., Cheung, A. K., Ko, J. M., Kan, R., Wong, B. W., Leong, M. M., Deng, M., Kwok, T. C., Chan, J. Y., Kwong, D. L., Lee, A. W., Ng, W. T., Ngan, R. K., Yau, C. C., *et al.* (2016) Whole-exome sequencing identifies multiple loss-of-function mutations of NF-κB pathway regulators in nasopharyngeal carcinoma. *Proc. Natl. Acad. Sci. U.S.A.* **113,** 11283–11288 CrossRef Medline
11. Bei, J. X., Li, Y., Jia, W. H., Feng, B. J., Zhou, G., Chen, L. Z., Feng, Q. S., Low, H. Q., Zhang, H., He, F., Tai, E. S., Kang, T., Liu, E. T., Liu, J., and Zeng, Y. X. (2010) A genome-wide association study of nasopharyngeal carcinoma identifies three new susceptibility loci. *Nat. Genet.* **42,** 599–603 CrossRef Medline
12. Lin, D. C., Meng, X., Hazawa, M., Nagata, Y., Varela, A. M., Xu, L., Sato, Y., Liu, L. Z., Ding, L. W., Sharma, A., Goh, B. C., Lee, S. C., Petersson, B. F., Yu, F. G., Macary, P., *et al.* (2014) The genomic landscape of nasopharyngeal carcinoma. *Nat. Genet.* **46,** 866–871 CrossRef Medline
13. Dai, W., Zheng, H., Cheung, A. K., Tang, C. S., Ko, J. M., Wong, B. W., Leong, M. M., Sham, P. C., Cheung, F., Kwong, D. L., Ngan, R. K., Ng,

ASBMB

W. T., Yau, C. C., Pan, J., Peng, X., *et al.* (2016) Whole-exome sequencing identifies MST1R as a genetic susceptibility gene in nasopharyngeal carcinoma. *Proc. Natl. Acad. Sci. U.S.A.* **113,** 3317–3322 CrossRef Medline

14. Ke, L., Zhou, H., Wang, C., Xiong, G., Xiang, Y., Ling, Y., Khabir, A., Tsao, G. S., Zeng, Y., Zeng, M., Busson, P., Kieff, E., Guo, X., and Zhao, B. (2017) Nasopharyngeal carcinoma super-enhancer-driven ETV6 correlates with prognosis. *Proc. Natl. Acad. Sci. U.S.A.* **114,** 9683–9688 CrossRef Medline
15. Yuan, J., Jiang, Y. Y., Mayakonda, A., Huang, M., Ding, L. W., Lin, H., Yu, F., Lu, Y., Loh, T. K. S., Chow, M., Savage, S., Tyner, J. W., Lin, D. C., and Koeffler, H. P. (2017) Super-enhancers promote transcriptional dysregulation in nasopharyngeal carcinoma. *Cancer Res.* **77,** 6614–6626 CrossRef Medline
16. Ma, Y., Walsh, M. J., Bernhardt, K., Ashbaugh, C. W., Trudeau, S. J., Ashbaugh, I. Y., Jiang, S., Jiang, C., Zhao, B., Root, D. E., Doench, J. G., and Gewurz, B. E. (2017) CRISPR/Cas9 screens reveal Epstein-Barr virus-transformed B cell host dependency factors. *Cell Host Microbe* **21,** 580–591.e7 CrossRef Medline
17. Cheung, S. T., Huang, D. P., Hui, A. B., Lo, K. W., Ko, C. W., Tsang, Y. S., Wong, N., Whitney, B. M., and Lee, J. C. (1999) Nasopharyngeal carcinoma cell line (C666-1) consistently harbouring Epstein-Barr virus. *Int. J. Cancer* **83,** 121–126 CrossRef Medline
18. Li, H. M., Zhuang, Z. H., Wang, Q., Pang, J. C., Wang, X. H., Wong, H. L., Feng, H. C., Jin, D. Y., Ling, M. T., Wong, Y. C., Eliopoulos, A. G., Young, L. S., Huang, D. P., and Tsao, S. W. (2004) Epstein-Barr virus latent membrane protein 1 (LMP1) upregulates Id1 expression in nasopharyngeal epithelial cells. *Oncogene* **23,** 4488–4494 CrossRef Medline
19. Li, W., Xu, H., Xiao, T., Cong, L., Love, M. I., Zhang, F., Irizarry, R. A., Liu, J. S., Brown, M., and Liu, X. S. (2014) MAGeCK enables robust identification of essential genes from genome-scale CRISPR/Cas9 knockout screens. *Genome Biol.* **15,** 554 CrossRef Medline
20. Chen, C. H., Xiao, T., Xu, H., Jiang, P., Meyer, C. A., Li, W., Brown, M., and Liu, X. S. (2018) Improved design and analysis of CRISPR knockout screens. *Bioinformatics* **34,** 4095–4101 CrossRef Medline
21. Avvakumov, N., and Côté, J. (2007) The MYST family of histone acetyltransferases and their intimate links to cancer. *Oncogene* **26,** 5395–5407 CrossRef Medline
22. Yang, X. J. (2004) The diverse superfamily of lysine acetyltransferases and their roles in leukemia and other diseases. *Nucleic Acids Res.* **32,** 959–976 CrossRef Medline
23. Zhang, J., Jia, L., Lin, W., Yip, Y. L., Lo, K. W., Lau, V. M. Y., Zhu, D., Tsang, C. M., Zhou, Y., Deng, W., Lung, H. L., Lung, M. L., Cheung, L. M., and Tsao, S. W. (2017) Epstein-Barr virus-encoded latent membrane protein 1 upregulates glucose transporter 1 transcription via the mTORC1/NF-κB signaling pathways. *J. Virol.* **91,** e02168-16 Medline
24. Sasaki, K., and Iwai, K. (2015) Roles of linear ubiquitinylation, a crucial regulator of NF-κB and cell death, in the immune system. *Immunol. Rev.* **266,** 175–189 CrossRef Medline
25. Goh, A. M., Coffill, C. R., and Lane, D. P. (2011) The role of mutant p53 in human cancer. *J. Pathol.* **223,** 116–126 CrossRef Medline
26. Toledo, F., and Wahl, G. M. (2006) Regulating the p53 pathway: *in vitro* hypotheses, *in vivo veritas*. *Nat. Rev. Cancer* **6,** 909–923 CrossRef Medline
27. Baell, J. B., Leaver, D. J., Hermans, S. J., Kelly, G. L., Brennan, M. S., Downer, N. L., Nguyen, N., Wichmann, J., McRae, H. M., Yang, Y., Cleary, B., Lagiakos, H. R., Mieruszynski, S., Pacini, G., Vanyai, H. K., *et al.* (2018) Inhibitors of histone acetyltransferases KAT6A/B induce senescence and arrest tumour growth. *Nature* **560,** 253–257 CrossRef Medline
28. Thomas, T., and Voss, A. K. (2007) The diverse biological roles of MYST histone acetyltransferase family proteins. *Cell Cycle* **6,** 696–704 CrossRef Medline
29. Pérez-Salvia, M., and Esteller, M. (2017) Bromodomain inhibitors and cancer therapy: from structures to applications. *Epigenetics* **12,** 323–339 CrossRef Medline
30. French, C. A. (2016) Small-molecule targeting of BET proteins in cancer. *Adv. Cancer Res.* **131,** 21–58 CrossRef Medline
31. Yan, K., Rousseau, J., Littlejohn, R. O., Kiss, C., Lehman, A., Rosenfeld, J. A., Stumpel, C. T. R., Stegmann, A. P. A., Robak, L., Scaglia, F., Nguyen, T. T. M., Fu, H., Ajeawung, N. F., Camurri, M. V., Li, L., *et al.* (2017) Mutations in the chromatin regulator gene BRPF1 cause syndromic intellectual disability and deficient histone acetylation. *Am. J. Hum. Genet.* **100,** 91–104 CrossRef Medline
32. Raab-Traub, N. (2012) Novel mechanisms of EBV-induced oncogenesis. *Curr. Opin. Virol.* **2,** 453–458 CrossRef Medline
33. Rodriguez-Galindo, C., Wofford, M., Castleberry, R. P., Swanson, G. P., London, W. B., Fontanesi, J., Pappo, A. S., and Douglass, E. C. (2005) Preradiation chemotherapy with methotrexate, cisplatin, 5-fluorouracil, and leucovorin for pediatric nasopharyngeal carcinoma. *Cancer* **103,** 850–857 CrossRef Medline
34. Kwong, D. L., Sham, J. S., Au, G. K., Chua, D. T., Kwong, P. W., Cheng, A. C., Wu, P. M., Law, M. W., Kwok, C. C., Yau, C. C., Wan, K. Y., Chan, R. T., and Choy, D. D. (2004) Concurrent and adjuvant chemotherapy for nasopharyngeal carcinoma: a factorial study. *J. Clin. Oncol* **22,** 2643–2653 CrossRef Medline
35. Siu, L. L., Czaykowski, P. M., and Tannock, I. F. (1998) Phase I/II study of the CAPABLE regimen for patients with poorly differentiated carcinoma of the nasopharynx. *J. Clin. Oncol.* **16,** 2514–2521 CrossRef Medline
36. Sommermann, T. G., O'Neill, K., Plas, D. R., and Cahir-McFarland, E. (2011) IKKβ and NF-κB transcription govern lymphoma cell survival through AKT-induced plasma membrane trafficking of GLUT1. *Cancer Res.* **71,** 7291–7300 CrossRef Medline
37. Hrdinka, M., and Gyrd-Hansen, M. (2017) The Met1-linked ubiquitin machinery: emerging themes of (de)regulation. *Mol. Cell* **68,** 265–280 CrossRef Medline
38. Yip, Y. L., Lin, W., Deng, W., Jia, L., Lo, K. W., Busson, P., Vérillaud, B., Liu, X., Tsang, C. M., Lung, M. L., and Tsao, S. W. (2018) Establishment of a nasopharyngeal carcinoma cell line capable of undergoing lytic Epstein-Barr virus reactivation. *Lab. Invest.* **98,** 1093–1104 CrossRef Medline
39. Li, W., Köster, J., Xu, H., Chen, C. H., Xiao, T., Liu, J. S., Brown, M., and Liu, X. S. (2015) Quality control, modeling, and visualization of CRISPR screens with MAGeCK-VISPR. *Genome Biol.* **16,** 281 CrossRef Medline
40. Luo, W., and Brouwer, C. (2013) Pathview: an R/Bioconductor package for pathway-based data integration and visualization. *Bioinformatics* **29,** 1830–1831 CrossRef Medline
41. Anaya, J. (2016) OncoLnc: linking TCGA survival data to mRNAs, miRNAs, and lncRNAs. *PeerJ Comp. Sci.* **2,** e67 CrossRef